

INSTRUCTIONAL LABORATORIES AND DEMONSTRATIONS

John Essick, Editor

Department of Physics, Reed College, Portland, OR 97202

Articles in this section deal with new ideas and techniques for instructional laboratory experiments, for demonstrations, and for equipment that can be used in either. Although these facets of instruction also appear in regular articles, this section is for papers that primarily focus on equipment, materials, and how they are used in instruction. Manuscripts should be submitted using the web-based system that can be accessed via the American Journal of Physics home page, ajp.aapt.org, and will be forwarded to the IL&D editor for consideration.

Molecular spectroscopy as a laboratory experiment: Measurement of important parameters of sodium diatomic molecules

Md Shakil Bin Kashem, a) Morgan Davies, b) Lok Pant, c) and S. Burcin Bayramd) Miami University, Oxford, Ohio 45056

(Received 28 August 2022; accepted 8 August 2023)

We present an inexpensive sodium molecular spectroscopy experiment for use in an advanced undergraduate laboratory course in physics or chemistry. The molecules were excited predominantly from the ground $X^1\Sigma_n^+(v''=15)$ state to the $B^1\Pi_n(v'=6)$ state using a commercially available 532nm broadband diode laser. The laser-induced molecular fluorescence was measured using a miniature fiber-coupled spectrometer at a resolution of 0.5 nm. The spectral peak assignments were done by comparing the observed spectrum with the calculated Franck-Condon values. Important molecular constants such as fundamental frequency, anharmonicity, bond strength, and dissociation energy of the ground electronic state were determined by using the Birge-Sponer extrapolation method. The presence of highly visible blue glowing molecules along the green laser beam creates an engaging laboratory experience. Emphasis is placed on students developing their understanding of the molecular structure, practicing molecular spectroscopic techniques, and applying knowledge of light-matter interactions to a physical system. © 2023 Published under an exclusive license by American Association of Physics Teachers.

http://aapt.org/ajp

https://doi.org/10.1119/5.0123126

I. INTRODUCTION

Atomic spectroscopy is an important part of the physics advanced laboratory curriculum, but its counterpart, molecular spectroscopy, often receives scant attention in undergraduate programs. Nevertheless, the significance of spectroscopic analysis cannot be overstated, as it represents a highly useful and versatile tool for scientific research and has a broad range of applications across diverse disciplines, including chemistry, biology, and physics. 1-8 Unfortunately, the high cost of equipment can be a formidable obstacle for many undergraduate programs, impeding students' access to hands-on training and practical knowledge in this valuable field. Thus, it is essential to explore affordable and accessible molecular spectroscopy experiments that can provide students with a deeper understanding of this fundamental discipline.

Due to the rapidly expanding research field in ultracold molecular physics, molecular spectroscopy using diatomic alkali molecules has been at the forefront of quantum chemistry and many-body physics, since it seeks to better understand quantum systems through their interactions with light. Various types of lasers and techniques have been used to measure the fluorescence spectrum of sodium molecules and extract molecular constants with high precision. 10-15 In this work, we present an affordable molecular spectroscopy

experiment to obtain important parameters of the ground electronic state sodium diatomic molecules.

We used an inexpensive 532-nm broadband diode laser to induce the electronic transition from the $X^1\Sigma_{\sigma}^+$ state to the $B^1\Pi_u$ state in gas-phase sodium diatomic molecules. A laserinduced fluorescence spectrum was measured using a miniature fiber-coupled spectrometer at moderate resolution (0.5 nm). The spectral peaks were assigned by comparing them with the calculated Franck-Condon values. Using the Birge-Sponer extrapolation method, molecular constants such as the fundamental frequency, bond strength, anharmonicity, and dissociation energy of the $X^1\Sigma_g^+$ electronic state were deduced. The relevant potential energy curves 16 of diatomic sodium molecules as well as the excitation and observed emission scheme are shown in Fig. 1.

II. THEORETICAL BACKGROUND

A diatomic molecule, made of two atoms held together by a chemical bond, can vibrate and rotate, which gives it additional degrees of freedom compared to a single atom. Because of this, diatomic molecules have quantized electronic, vibrational, and rotational energy levels and exhibit dense spectra compared to atomic spectra. These special

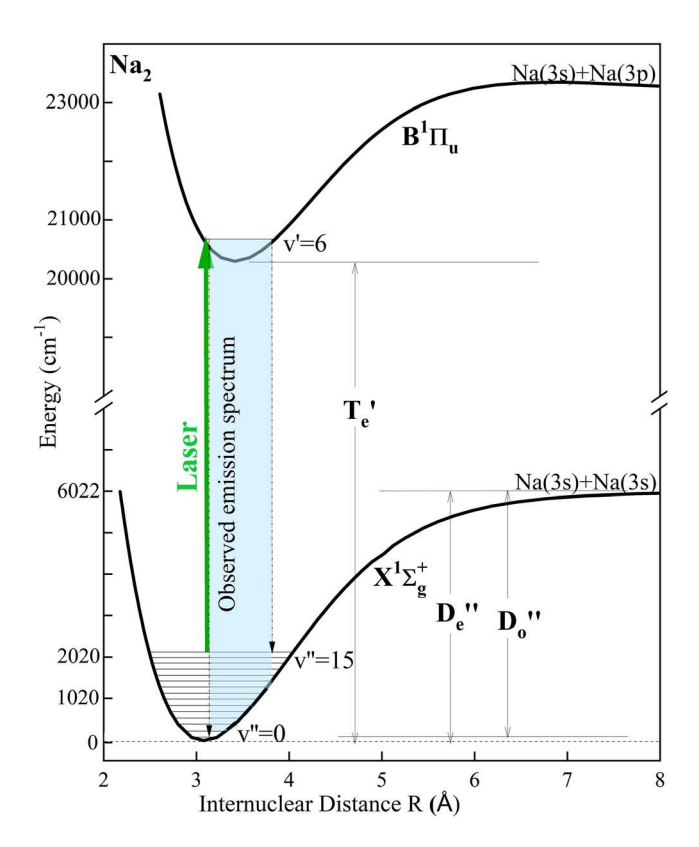


Fig. 1. The potential energy curves (Ref. 16) of the sodium molecules and the excitation scheme. The green broadband diode laser at $18\,789\,\mathrm{cm}^{-1}$ excites molecules predominantly from the $X^1\Sigma_g^+(v''=15)$ electronic state to the $B^1\Pi_u(v'=6)$ electronic state. The fluorescence (blue-shaded area) was collected with a miniature fiber-coupled spectrometer at a resolution of about 0.5 nm. Also shown are the dissociation energies D_e'' , D_o'' of the ground state, and the electronic term value T_e' . The energy zero is at the minimum of the ground-state potential (T'').

features of the molecules make them optimal candidates for research in molecular physics and quantum chemistry.

A diatomic molecule, consisting of two nuclei and two valence electrons, can be modeled within the Born–Oppenheimer approximation, in which the nuclei are considered stationary during an electronic transition. Hence, the total energy E of a diatomic molecule is expressed as the sum of electronic (E_e), vibrational (E_v), and rotational (E_J) energies. Here, v is the vibrational quantum number, and J is the rotational quantum number. In spectroscopic studies, it is customary to define energies in terms of wavenumbers (cm $^{-1}$), called term values, by dividing the energies by hc. Thus, the total energy can be written in terms of term values as

$$T(v,J) = T_e + G_v + F_v(J),$$
 (1)

where G_v and $F_v(J)$ are the vibrational and rotational term values, and T_e is the electronic term value, which is the energy of the minimum of the potential curve. In a diatomic molecule, the potential energy can be approximated by the Morse potential, ¹⁸

$$V(R) = D_e (1 - e^{-\beta(R - R_e)})^2,$$
 (2)

where R is the internuclear distance, R_e is the equilibrium internuclear distance (bond length), D_e is the dissociation energy given by the depth of the potential well, and β is

related to the force constant k_e (bond strength) as $\beta=(k_e/2D_e)^{1/2}$. The dissociation energy D_e is a measure of the strength of the chemical bond between the two atoms. It is the minimum amount of energy required to dissociate the molecule into its constituent atoms. Since diatomic molecules both rotate and vibrate, it is difficult to solve the three-dimensional Schrödinger equation for the Morse potential. Thus, an approximate solution for the vibrational energy eigenvalue of the one-dimensional Schrödinger equation with the assumption that the rotation does not occur can be written as ¹⁸

$$G_v = \omega_e \left(v + \frac{1}{2} \right) - \omega_e \chi_e \left(v + \frac{1}{2} \right)^2, \tag{3}$$

where ω_e is the fundamental frequency of the vibration, and $\omega_e \chi_e$ is the first-order energy deviation from that of a harmonic oscillator, called the anharmonicity constant. The vibrational energy G_v is still non-zero at the lowest v; this energy is called zero-point energy. When the vibrational energy exceeds D_e , the diatomic molecule is no longer bound, the bond breaks, and it dissociates into two atoms.

A diatomic molecule can be modeled as a rigid rotator, which reasonably describes the rotational energy levels of a molecule. For a rigid rotator, the separation between the nuclei must be constant. However, in reality, as J gets larger, the molecule rotates faster, which results in a larger internuclear separation and a larger moment of inertia. The energy of a rotational level within a vibrational level can be expressed as

$$F_v(J) = B_v J(J+1) - D_v J^2 (J+1)^2, \tag{4}$$

where B_v is the vibrational state dependence of the rotational constant, which is expressed as $B_v = B_e + \alpha_e(v+1/2)$, with B_e and α_e being the equilibrium rotational and vibrational-rotational coupling constants, respectively, and D_v is the centrifugal distortion constant that is responsible for the decrease in the rotational energy of the rigid rotator as the molecule stretches for large J. The magnitude of the rotational constant, which varies with different v, is a measure of the energy spacing between two rotational levels. For instance, the energy difference between a level J and the next higher level, J+1, is approximately $2JB_v$.

In any real molecule, rotation and vibration occur simultaneously and thus it exhibits rotational–vibrational (rovibrational) energy levels. Conventionally, the quantum numbers for the ground electronic state are labeled with a double prime, whereas those for the upper electronic state are labeled with a single prime. Thus, total energy change in a transition between a ground electronic state with v'', J'' and an excited electronic state with v', J' can be written as

$$\tilde{\nu}_{v'v''J'J''} = T(v',J') - T(v'',J''). \tag{5}$$

In this experiment, the rotational structure cannot be resolved due to the low resolution of the spectrometer; thus, a transition between two vibrational levels can be re-written

$$\tilde{\nu}_{v'v''} = \tilde{\nu}_{el} + (G_{v'} - G_{v''}),\tag{6}$$

where $\tilde{\nu}_{el}=T'_e-T''_e=T'_e$ since $T''_e=0$ for the ground electronic state. Since there is no selection rule for the

vibrational quantum number, any v' can be combined with any v''; thus, a large number of spectral lines (bands) can be observed.

The spectroscopic notation for the electronic states of diatomic molecules is represented by $^{2S+1}\Lambda_{\Omega}^{\pm}$, similar to notation used for atomic states $^{2S+1}L_J$, where S is the total spin, J is the total angular momentum, and L is the total orbital angular momentum quantum numbers. In molecular spectroscopy, the symbol J designates the rotational quantum number. The multiplicity is (2S+1), and the values Ω and Λ are the projections of the total angular and orbital momenta along the internuclear axis, respectively. The quantum number Ω is appended with the subscript g as gerade or u as ungerade to indicate the parity of the molecular state, which depends on whether the wavefunction remains unchanged upon reflection through the center of the molecule. 19 Thus, $\Lambda = 0$ is called a Σ state, $\Lambda = 1$ is a Π state, and so forth. The superscript ± defines the symmetry and applies to molecules in Σ states only. For the ${}^{1}\Sigma \leftrightarrow {}^{1}\Sigma$ electronic transition $(\Delta \Lambda = 0)$, the allowed rotational transitions are $\Delta J = \pm 1$, and for the ${}^{1}\Sigma \leftrightarrow {}^{1}\Pi$ electronic transitions ($\Delta\Lambda = \pm 1$), the allowed rotational transitions are $\Delta J = -1, 0, +1$. These are referred to as the P, Q, and R branches, respectively. A selectively excited rovibrational level, which consists of triplet branches in the Π state, emits on $\Pi \to \Sigma$ transitions, either only Q or only P and R branches, depending on the symmetry of the rotational levels.²⁰

The intensity of an emission spectrum can be analyzed by comparing the experimental peaks with the theoretical values. Relative intensity of a transition between any two vibrational levels is proportional to the square of the vibrational wave functions' overlap integral,

$$I \propto \left| \int (\psi_{v'}^*)(\psi_{v''}) dR \right|^2,$$
 (7)

which is known as the Franck–Condon factor (FCF). Transitions with large overlap between the ground and excited state wave functions give high intensity peaks in the spectra. To calculate the FCFs for the $B^1\Pi_u(v'=5) \rightarrow X^1\Sigma_g^+(v'')$ transition, we use a computer program, which is called LEVEL 8.0. 23,24 This program, adaptable to any molecule, solves the radial Schrödinger equation for bound and quasi-bound potential levels to calculate the Franck–Condon factors, energies, and other characteristics. To run the program, we created an input text file, which has the information about the sodium molecule and its experimentally determined potential energy curves 25,26 for the $X^1\Sigma_g^+$ and $B^1\Pi_u$ electronic states. We then identify the observed spectral band by comparing them with the output of the program.

The intensity of a spectral line not only depends on FCF but also on the number of molecules in the various rovibrational levels of the electronic ground state. Since we observe emission spectra at thermal equilibrium, it is necessary to consider the relative population distribution of molecules at 380° C, the operating temperature of the oven. The population of any v'' level, at thermal equilibrium, is proportional to the Boltzmann factor as $N(v'') \propto \exp(-G_{v''}/(k_BT))$, where k_BT is the thermal energy (in cm⁻¹). The number of molecules in the J'' level of the lowest vibrational level is proportional as follows: $N(J'') \propto g_J \exp(-F_v(J'')/(k_BT))$, where $g_J = 2J'' + 1$ is the degeneracy. Figure 2 represents graphically the relative population distribution in various v'' and J''.

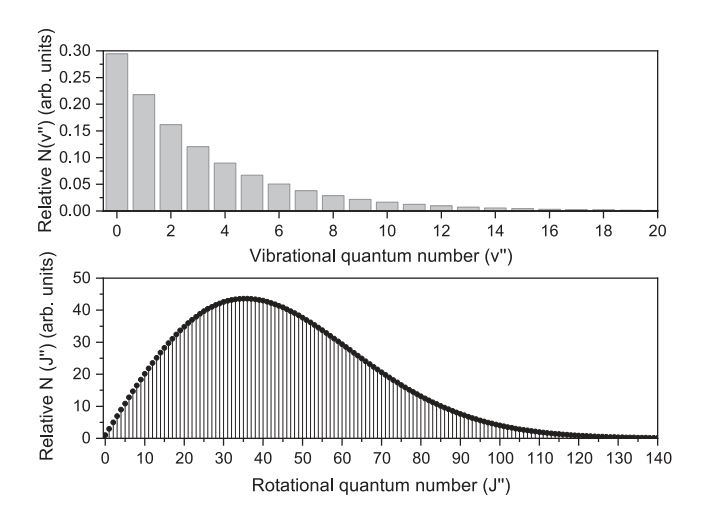


Fig. 2. Relative population distribution of sodium molecules in the vibrational and rotational levels of the $X^1\Sigma_g^+$ ground electronic state at 380 °C, and $B_e^{~27} = 0.1547 \, \mathrm{cm}^{-1}$.

The population, at 380 °C, in v''=14 relative to v''=0, is about 3%. The population of the various J'' levels are calculated at T=380 °C and $B_e^{27}=0.1547$ cm⁻¹ (the vibrational state dependence of the rotational constant $B_v\approx B_e$ is neglected).

Homonuclear molecules like Na₂ have no permanent dipole moment; thus, they do not absorb or emit radiation on transitions within the same electronic state. The Na₂ molecule consists of two ²³Na atoms having half-odd-integer spin (I=3/2) each. Thus, the sodium nuclei are fermions and obey Pauli Exclusion principle, which requires that the total wave function of the molecule must be antisymmetric. There are a total of $(2I+1)^2 = 16$ ways to combine the spins on the two sodium nuclei. The possible values of the total nuclear spin combinations (I = 3, 2, 1, and 0) give ten antisymmetric nuclear-spin wavefunctions, which form ortho-states (I = 1,3; nuclear spin weight $g_N = 10$), and six symmetric nuclearspin wavefunctions, which form para-states (I = 2, 0; nuclear spin weight $g_N = 6$). Hence, for the total wavefunction to be antisymmetric, the antisymmetric rotational levels (odd-J) of the ground electronic state will combine with the ortho nuclear spin configurations, while symmetric rotational levels (even-J) of the ground electronic state will combine with the para nuclear spin states. 19,28–31 The symmetry of the total molecular wave function remains constant with respect to nuclear exchange. It is for this reason that when the molecules are formed in the heat-pipe oven, a mixture of odd-J and even-J configurations are formed, and thus all J levels of the ground electronic state are populated as shown in Fig. 2.

III. EXPERIMENTAL SETUP

The experimental setup is shown in Fig. 3. The heat-pipe oven^{32–36} consists of an air-tight stainless steel tube, which has a length of one meter, and four arms for the beam entrance and exit windows and the observation and detection windows. Optical cell designs are also used to create gasphase alkali molecules.^{37,38} The sodium metal is placed in the center of this oven. After evacuating the oven until the background pressure is 15 mTorr using a mechanical pump, argon is introduced into the oven as a buffer gas. The gas valve is closed to keep a fixed amount of argon gas at 150 mTorr at room temperature inside the oven. The heat-pipe oven is then heated by four pairs of non-magnetic

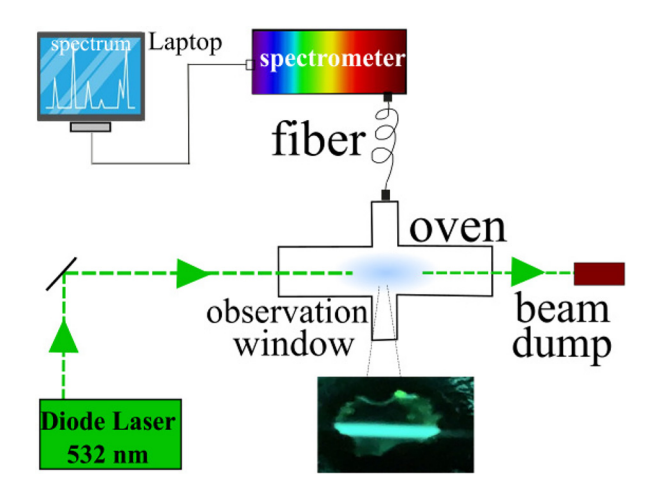


Fig. 3. Schematic of the experimental setup is shown. The sodium molecular vapor is formed inside the heat-pipe oven at 380 °C with 150 mTorr argon buffer gas. Molecules are excited to the $B^1\Pi_u$ state by the green broadband diode laser operating at 20 mW. LIF is collected at right angles to the laser's propagation direction using a fiber-coupled miniature spectrometer. The inset shows a photograph of the blue glowing molecules along the laser beam through the observation window, taken with a cell phone camera.

ceramic heaters to a sufficient temperature, at least $300\,^{\circ}\text{C}$. The oven is covered with a ceramic fiber blanket and aluminum foil to maintain a homogenous temperature inside the oven. At the same time, cold water is run through copper coils wrapped near the windows of the arms so that the stainless steel mesh lining at the arms of the oven walls acts as a wick to return the liquid metal back to the central region of the oven to prevent condensation onto the windows. At about $380\,^{\circ}\text{C}$ estimated atomic and molecular number densities are on the order of 10^{14} and $10^{12}\,\text{cm}^{-3}$, respectively.

on the order of 10^{14} and 10^{12} cm⁻³, respectively.³⁹ We used a broadband diode laser (BBDL)⁴⁰ operating at 532 nm with 20 mW power and 60 GHz (2 cm⁻¹) bandwidth to excite sodium molecules from the $X^1\Sigma_g^+(v''=15)$ state to the $B^1\Pi_u(v'=6)$ state. The excited molecules relax to a range of vibrational levels in the ground state, yielding a laser-induced fluorescence (LIF) spectrum spanning 470–560 nm range. Thus, the blue glowing molecules can be readily observed by the naked eye from the observation window of the oven, as seen in Fig. 3.

The LIF spectrum was collected perpendicular to the laser's propagation direction using a miniature fiber-coupled spectrometer⁴¹ with moderate resolution (0.5 nm). The spectrum was recorded at 20 s integration time with background correction. From the spectral analysis, we extracted the important molecular constants for the ground electronic state of sodium molecules. For comparison of the results, we repeated the experiment using a narrowband diode laser (NBDL)⁴⁰ operating at 532 nm with a bandwidth of 5 MHz. The power of the NBDL was kept at 20 mW to match the BBDL's power, and molecular fluorescence was captured using the same spectrometer for a better comparison. To ensure that the wavelengths of the measured spectrum are correctly labeled and aligned with the correct intensity values, we calibrated the spectrum using He light source.42 Comparing the measured spectrum with the He spectral lines at 447.15 and 587.56 nm, we found 0.44 and 0.76 nm deviations, respectively. A linear fit to the deviations against the measured wavelengths gives a calibration function. We used this function to correct the measured wavelengths. Additionally, we used a Coherent wavemeter, which has an

internal calibration system based on precisely known wavelengths of neon spectral lines, to measure the wavelengths of the lasers. The wavelength of the BBDL is measured as 18 789 cm⁻¹ (532.24 nm). Then, we compared this value with the wavelength of the laser line in the corrected spectrum and found 0.07 nm difference. The NBDL wavelength is measured using a wavemeter, which is 18 791 cm⁻¹ (532.17 nm), and the difference between this value and the corrected NBDL spectrum is 0.35 nm.

IV. RESULTS AND DISCUSSION

A. Spectral peak assignment

Figure 4 shows the LIF spectra, recorded using both NBDL and BBDL, and the calculated Franck–Condon factors. The vibrational progression of the $B^1\Pi_u$ electronic state was observed in both spectra. To identify correct excitation pathways for both spectra, we calculated FCFs for the combinations of all transitions between $B^1\Pi_u(v', J' = J'', J'' \pm 1)$ and $X^1\Sigma_g^+(v'', J'')$ states, where v'' = 0–16, v' = 0–16, and J'' = 19–42, and compared the results with the observed spectra. The intensities of the observed spectral peaks labelled as "laser line" are artificially enhanced from the Rayleigh scattering; thus, their FCFs are smaller than the spectra suggest.

For the 5 MHz bandwidth of the NBDL laser operating at 532.17 nm (18791 cm⁻¹), we identified a single excitation pathway: P(39) line of the $B^1\Pi_u(v'=5) \leftarrow X^1\Sigma_g^+(v''=14)$ transition. The relative intensity pattern of the observed spectrum is strongly correlated with the $B^1\Pi_u(v'=5)$ relaxation if the spectral peaks are compared with the computed FCFs in Table I. For the 60 GHz bandwidth of the BBDL laser operating at 532.24 nm (18789 cm⁻¹), we identified three excitation pathways:⁴³ Q(33) and Q(34) lines of the $B^1\Pi_u(v'=6) \leftarrow X^1\Sigma_g^+(v''=15)$ transition, and P(39) line of the $B^1\Pi_u(v'=5) \leftarrow X^1\Sigma_g^+(v''=14)$ transition. The agreement between the observed intensity pattern and the computed FCFs is more favorable for the relaxation of the $B^1\Pi_u(v'=6)$ state than that of the $B^1\Pi_u(v'=5)$ state when comparing with the tabulated FCFs in Table II. For example, the assignment of the peaks v'' = 3, 5, 7, 9, 10, 11, and 12–16 in the observed spectrum shows strong agreement with the $B^1\Pi_u(v'=6)$ relaxation. This is further supported by the absence of the peak at 477.06 nm from the $B^1\Pi_u(v'=5)$ relaxation. However, the BBDL spectrum is likely a mix of emissions from the $B^1\Pi_u(v'=6)$ and $B^1\Pi_u(v'=5)$ relaxations following excitation from both the $X^1\Sigma_a^+(v''=14)$ and $X^1\Sigma_a^+(v''=15)$ states. For example, in the BBDL spectrum, the spectral peaks v'' = 2, 4, and 6 are enhanced as a result of the contribution from the peaks v'' = 1, 3, and 5 of the $B^1\Pi_u(v'=5)$ relaxation. The enhancement of the peak v'' = 17 is unlikely from the B ${}^{1}\Pi_{u}(v' = 5)$ relaxation due to the low FCF. Therefore, the peak v'' = 17 is excluded from the spectral analysis. The spectral assignment of the peaks corresponding to v'' = 18, 19, and 20, proved elusive, and as a result, these peaks were excluded from the analysis.

The FCFs for the $B^1\Pi_u(v'=0-10) \to X^1\Sigma_g^+(v''=0-23)$ transitions for J=0 are reported. Our calculated FCFs are consistent with the reported values. Since rotational lines are not resolved in the observed spectra, we averaged FCFs and corresponding wavelengths for each vibrational peak of the $B^1\Pi_u(v'=6) \to X^1\Sigma_g^+(v''=15)$ for Q(33) and Q(34) transitions. This allows us to make a more realistic comparison

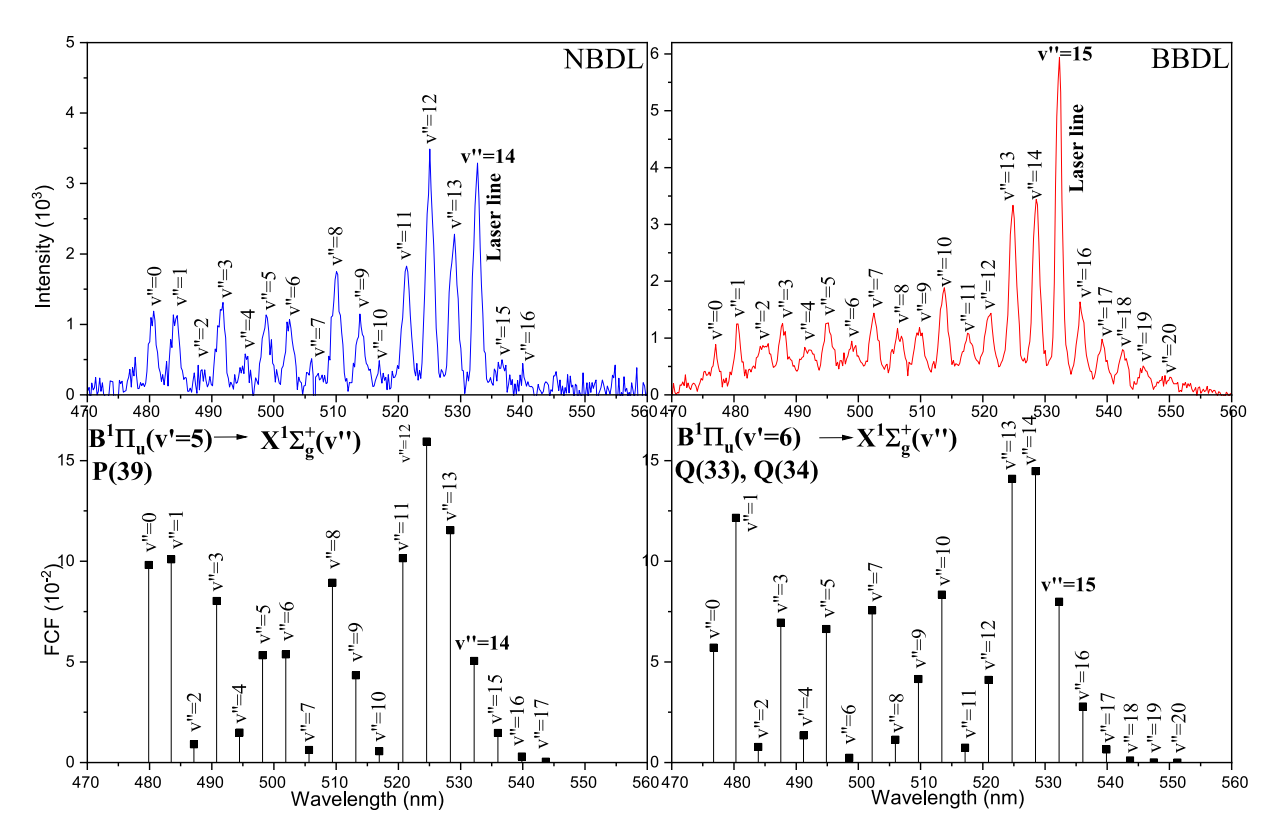


Fig. 4. LIF spectrum using NBDL and calculated FCF spectrum for the P(39) line of the $B^1\Pi_u(v'=5) \to X^1\Sigma_g^+(v'')$ transition (left), and LIF spectrum using BBDL and calculated FCF spectrum, averaged for the Q(33) and Q(34) lines of the $B^1\Pi_u(v'=6) \to X^1\Sigma_g^+(v'')$ transition (right). In both spectra, recorded using a miniature fiber-coupled spectrometer at a resolution of 0.5 nm, vibrational progressions from the laser lines to v''=0 are observed.

between the experimentally obtained BBDL spectrum and the theoretically predicted FCF spectrum. Thus, Table II shows the average values of the Q(33) and Q(34) lines of each vibrational band. To estimate the wavelengths of the spectral peaks in the observed spectrum, we isolated the

Table I. Spectral peak wavelengths for the NBDL spectrum and the calculated FCFs for the P(39) line of the $B^1\Pi_u(v'=5) \to X^1\Sigma_{\varphi}^+(v'')$ transition.

v'	v''	$\tilde{\nu}_{v'v''} (\text{cm}^{-1})$ Theory	FCF	λ (nm) Theory	$\lambda \pm 0.7 \text{ (nm)}$ NBDL
5	17	18 393	4.21×10^{-4}	543.68	_
5	16	18 524	2.97×10^{-3}	539.84	539.98
5	15	18 657	1.47×10^{-2}	536.01	536.66
5	14	18791	5.04×10^{-2}	532.17	532.52
5	13	18 927	1.15×10^{-1}	528.35	528.79
5	12	19 065	1.59×10^{-1}	524.53	525.05
5	11	19 204	1.02×10^{-1}	520.73	521.31
5	10	19 345	5.62×10^{-3}	516.94	517.17
5	9	19 487	4.34×10^{-2}	513.15	513.80
5	8	19631	8.93×10^{-2}	509.39	509.96
5	7	19777	6.28×10^{-3}	505.63	506.07
5	6	19924	5.37×10^{-2}	501.90	502.30
5	5	20 073	5.33×10^{-2}	498.18	498.74
5	4	20 224	1.49×10^{-2}	494.47	495.02
5	3	20 375	8.03×10^{-2}	490.79	491.43
5	2	20 529	9.08×10^{-3}	487.12	487.19
5	1	20 683	1.01×10^{-1}	483.48	484.02
5	0	20 840	9.81×10^{-2}	479.85	480.44

Table II. Spectral peak wavelengths for the BBDL spectrum, and the average values of the calculated FCFs for the Q(33) and Q(34) lines of the $B^1\Pi_u(v'=6) \to X^1\Sigma_g^+(v'')$ transition. The observed spectral peaks corresponding to wavelengths marked with (*), not anticipated to appear, and with (†), unexpectedly large, are excluded from the analysis.

v'	v''	$\tilde{\nu}_{v'v''} (\mathrm{cm}^{-1})$ Theory	FCF	λ (nm) Theory	$\lambda \pm 0.8 \text{ (nm)}$ BBDL
6	20	18 140	8.87×10^{-6}	551.28	549.56*
6	19	18 266	1.18×10^{-4}	547.48	545.83*
6	18	18 393	1.065×10^{-3}	543.68	542.56*
6	17	18 523	6.54×10^{-3}	539.87	539.26 [†]
6	16	18 654	2.79×10^{-2}	536.07	535.73
6	15	18 787	7.99×10^{-2}	532.27	532.31
6	14	18 922	1.45×10^{-1}	528.48	528.58
6	13	19 059	1.41×10^{-1}	524.70	524.84
6	12	19 197	4.11×10^{-2}	520.93	520.85
6	11	19336	7.39×10^{-3}	517.16	517.59
6	10	19 478	8.34×10^{-2}	513.41	513.74
6	9	19621	4.15×10^{-2}	509.67	509.83
6	8	19765	1.14×10^{-2}	505.94	506.44
6	7	19911	7.56×10^{-2}	502.23	502.48
6	6	20 059	2.39×10^{-3}	498.53	498.84
6	5	20 208	6.63×10^{-2}	494.85	495.08
6	4	20 359	1.35×10^{-2}	491.19	491.77
6	3	20511	6.95×10^{-2}	487.54	487.81
6	2	20 665	7.78×10^{-3}	483.92	484.73
6	1	20820	1.22×10^{-1}	480.31	480.61
6	0	20 977	5.71×10^{-2}	476.72	477.06

Table III. From Tables I and II, the spectral peak wavelengths for NBDL and BBDL are converted to wavenumbers, labelled as $\tilde{\nu}_{v'v'}$. The differences $\Delta G_{v''}$ between all adjacent vibrational energy levels v'' and v''+1 are tabulated. The column $\tilde{\nu}_{v'v''}$ has uncertainties within \pm 30 cm $^{-1}$, and the column $\Delta G_{v''}$ has uncertainties within \pm 43 cm $^{-1}$.

v''	v"+1	$\tilde{\nu}_{v'v''}$ (cm ⁻¹) (NBDL)	$\Delta G_{v''} \text{ (cm}^{-1})$ (NBDL)	$\tilde{\nu}_{v'v''}$ (cm ⁻¹) (BBDL)	$\Delta G_{v''} \text{ (cm}^{-1})$ (BBDL)
16	17	18 519		18 666	122
15	16	18 634	115	18 786	120
14	15	18 779	145	18919	133
13	14	18 911	133	19 053	135
12	13	19 046	135	19 199	146
11	12	19 182	137	19 320	121
10	11	19 336	154	19 465	145
9	10	19 463	127	19614	149
8	9	19 609	147	19746	131
7	8	19 760	151	19 901	156
6	7	19 908	148	20 047	145
5	6	20 05 1	142	20 199	152
4	5	20 201	151	20 335	136
3	4	20 349	148	20 500	165
2	3	20 526	177	20630	130
1	2	20 660	134	20 807	177
0	1	20 814	154	20 962	155

individual peak and determined the center of its base-width. The measurement error in the wavelength estimation is about ± 0.7 nm.

A systematic effect may arise from the fact that the hot heat-pipe oven is a non-equilibrium system. The thermal energy k_BT of the system is about $454 \,\mathrm{cm}^{-1}$, which is a few vibrational separations, e.g., v'' = 14-13 (see Table I) is about $136 \,\mathrm{cm}^{-1}$. Thus, collision-induced transitions with Na, Na₂, and buffer gas may populate other rovibrational energy levels, which then emit fluorescence and contribute additional spectral features to the spectrum.

B. Analysis of spectra

The vibrational term value in Eq. (3) can be used to extract spectroscopic constants of the Na₂ $X^1\Sigma_g^+$ ground electronic state by using the Birge–Sponer method. The

Birge–Sponer approach requires the subtraction of the energies for transitions originating from the same excited vibrational level of the $B^1\Pi_u(v'=5)$ state into the ground state of successive vibrational levels v''. Thus, the vibrational energy spacing between consecutive vibrational levels in the ground state can be written as

$$\Delta \tilde{\nu}_{v''} = G_{v''+1} - G_{v''} = \omega_e - 2\omega_e \chi_e(v''+1), \tag{8}$$

where $\Delta \tilde{\nu}_{v''} = \tilde{\nu}_{v'v''} - \tilde{\nu}_{v'v''+1}$. This result suggests that the energy spacings decrease linearly. Thus, the Birge–Sponer extrapolation method uses a plot of $\Delta \tilde{\nu}_{v''} = \Delta G_{v''}$ against (v''+1). Then, a linear fit to the data finds the intercept (ω_e) and slope $(-2\,\omega_e\chi_e)$. To find D_o'' with respect to the zeropoint level, the area under the linear plot in the v''=0 and v''_{\max} interval is estimated. Table III shows the values of $G_{v''}$ for each vibrational quantum number and its corresponding $\Delta G_{v''}$.

The Birge–Sponer plots for NBDL and BBDL are shown in Fig. 5. From the linear fit to the data, we found $\omega_e=158\pm6$ and $\omega_e\chi_e=0.86\pm0.32\,\mathrm{cm}^{-1}$ for the NBDL and $\omega_e=161\pm6$ and $\omega_e\chi_e=1.05\pm0.30\,\mathrm{cm}^{-1}$ for the BBDL. These values agree with the literature values for $\omega_e=159.18$ and $\omega_e\chi_e=0.76\,\mathrm{cm}^{-1}$ within the error limits. The result of regression analysis are shown on the plots. The effective force constant (bond strength) can be calculated from the relation $k_e=\mu(2\pi c\omega_e)^2$, where c is the speed of light in cm/s units and the reduced mass of the Na₂ molecule is $\mu=190.879\times10^{-28}\,\mathrm{kg}$ (11.495 amu). Therefore, the force constant is determined to be $k_e=16.9\pm1.3\,\mathrm{N/m}$ for NBDL and $k_e=17.6\pm1.4\,\mathrm{N/m}$ for BBDL.

Given the known vibrational spacing as depicted in Fig. 5, one can estimate the value of D_o'' by calculating the sum of all vibrational spacings from v''=0 to v''_{\max} . This calculation can be represented by finding the area under the red linear curve. Thus, the area of the triangle yields

$$D_o'' = \frac{\omega_e^2}{4\omega_e \gamma_e}. (9)$$

Combining Eq. (9) with Eq. (3), the dissociation energy D_e'' relative to the equilibrium point can be estimated. Thus, the dissociation energy of the ground electronic state can be approximated as

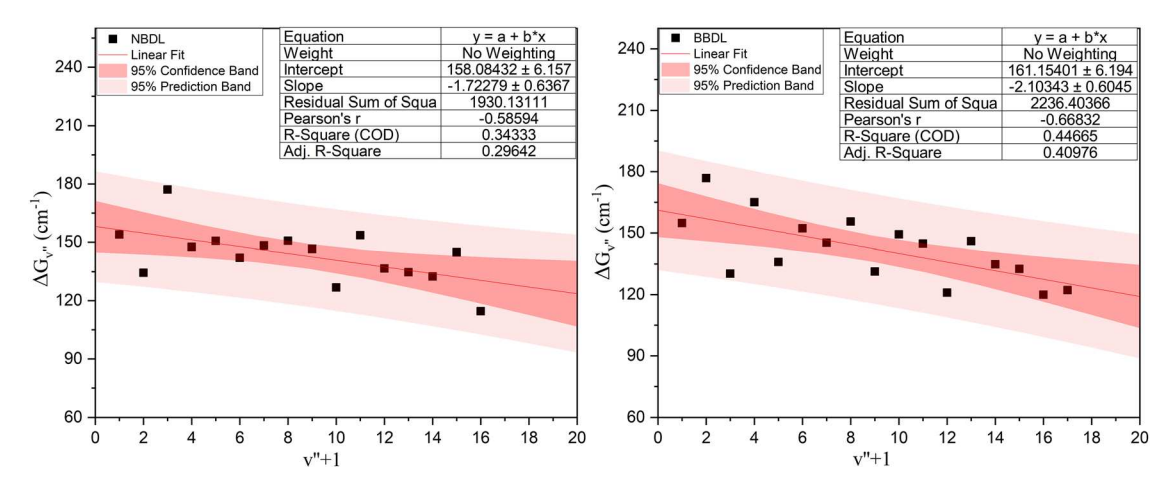


Fig. 5. Birge–Sponer extrapolation to deduce the molecular constants for the ground electronic state of Na₂ for the NBDL (left) and BBDL (right) spectra. All measured differences $\Delta G_{v''}$ vs v''+1 are plotted, and the dissociation energy, which is the area under the triangle between the lowest v''=0 and highest v''_{max} bound level, is estimated by linear extrapolation.

Table IV. The molecular constants for the $X^1\Sigma_o^+$ electronic state of Na₂ obtained from this work and their reported values in literature are tabulated.

Molecular constants	Literature	This work with NBDL	This work with BBDL
Fundamental frequency, ω_e	159.18 ^a cm ⁻¹	$158 \pm 6 \mathrm{cm}^{-1}$	$161 \pm 6 \mathrm{cm}^{-1}$
Anharmonicity, $\omega_e \chi_e$	0.76 ^a cm ⁻¹	$0.86 \pm 0.32 \mathrm{cm}^{-1}$	$1.05 \pm 0.30 \mathrm{cm}^{-1}$
Force constant, k_e	17 ^a N/m	$16.9 \pm 1.3 \text{ N/m}$	$17.6 \pm 1.4 \text{ N/m}$
Dissociation energy, D_o''	5944 ^a cm ⁻¹	$7300 \pm 2700^{\circ} \text{ cm}^{-1}$	$6200 \pm 1800^{\circ} \text{ cm}^{-1}$
Dissociation energy, D'_e	5988 ^b cm ⁻¹	$7300 \pm 2700^{\circ} \text{ cm}^{-1}$	$6300 \pm 1800^{\circ} \text{ cm}^{-1}$

^aReference 27.

$$D_e'' = D_o'' + \frac{1}{2}\omega_e - \frac{1}{4}\omega_e \chi_e.$$
 (10)

Using Eqs. (9) and (10), we found $D_0'' = 7300 \pm 2700$ and $D_e'' = 7300 \pm 2700 \,\mathrm{cm}^{-1}$ for the NBDL, and $D_o'' = 6200$ \pm 1800 and $D_e'' = 6300 \pm 1800 \,\mathrm{cm}^{-1}$ for the BBDL. Here, the level of precision ends at the hundreds place. The value of D_e'' remains poorly determined, since even the v'' = 17level is less than halfway to the dissociation limit. As a result of the limited number of measurable peaks in this type of experiment and the necessary linear approximation, the dissociation energy calculated using this method is often an overestimation of the actual value obtained through direct measurement. The literature values 26,27 for D_o'' and D_e'' are 5944 and 5988 cm $^{-1}$, respectively. All molecular parameters deduced from the observed spectrum and their literature values are summarized in Table IV.

V. CONCLUSION

We presented a molecular sodium spectroscopy experiment, which can be easily replicated using affordable equipment, provides students with valuable knowledge and understanding of molecular physics and applications, as well as important spectroscopic techniques. The green laser beam creates strikingly vivid blue glowing molecules that enhance the laboratory experience, capturing students' interest and inspiring them to explore molecular quantum systems through their interactions with electromagnetic radiation.

This study investigated the spectroscopy of molecular sodium in gas phase using an inexpensive 532-nm broadband diode laser, which predominantly excites the $B^1\Pi_u(v'=6)$ electronic state, and a miniature fiber-coupled spectrometer for detecting the LIF spectrum for the $B^1\Pi_u(v'=6)$ \rightarrow $X^1\Sigma_q^+(v''=15)$ transition. The molecular constants of the ground electronic state of Na₂, deduced from the spectrum using a broadband diode laser, were compared to those utilizing a narrow-band diode laser. Although the narrow-band diode laser provided a cleaner spectrum, results indicated that the affordable equipment provided accurate values within error limits, comparable to those obtained with more expensive options. This provides opportunities for advanced laboratory classes in chemistry and physics, which are potentially limited by a lack of resource availability. In many laboratory classes, experiments are limited to working with I₂ because it is easier to work with. While these experiments can provide insights into the molecular structure, the use of other compounds has the potential to enable students to compare and contrast the structures of diverse molecules, thus

facilitating a deeper comprehension of light-matter interactions.

Furthermore, analyzing the LIF spectrum and extracting the molecular properties of the electronic state of diatomic molecules can enable students to construct a potential energy curve using the Rydberg-Klein-Rees (RKR) method, 47which could serve as a future experiment in a larger project such as an undergraduate thesis.

ACKNOWLEDGMENTS

Financial support from the National Science Foundation (Grant Nos. NSF PHY-1607601 and PHY-2309340) is gratefully acknowledged. The authors are grateful to Chuck Williamson of Willamette University, Ergin Ahmed, and Marjatta Lyyra of Temple University and two anonymous referees for providing valuable suggestions and detailed comments that have enhanced the overall clarity of the work.

AUTHOR DECLARATIONS

Conflict of Interest

The authors have no conflicts to disclose.

^bReference 26.

^cThe precision ends at the hundreds place.

a)ORCID: 0000-0001-8400-0099.

b)ORCID: 0000-0002-5723-9448.

c)ORCID: 0000-0003-2492-3638.

d)Author to whom correspondence should be addressed: bayramsb@ miamioh.edu, ORCID: 0000-0003-3995-3186.

¹M. Terrell and M. F. Masters, "Laser spectroscopy of the cesium dimer as a physics laboratory experiment," Am. J. Phys. 64(9), 1116–1120 (1996).

²B. L. Sands, M. J. Welsh, S. Kin, R. Marhatta, J. D. Hinkle, and S. B. Bayram, "Raman scattering spectroscopy of liquid nitrogen molecules: An advanced undergraduate physics laboratory experiment," Am. J. Phys. **75**(6), 488–495 (2007).

³J. C. Williamson, "Teaching the rovibronic spectroscopy of molecular iodine," J. Chem. Educ. 84(8), 1355–1359 (2007).

⁴J. Blue, S. B. Bayram, and D. Marcum, "Creating, implementing, and sustaining an advanced optical spectroscopy laboratory course," Am. J. Phys. 78(5), 503–509 (2010).

⁵S. B. Bayram and M. V. Freamat, "Vibrational spectra of N₂: An advanced undergraduate laboratory in atomic and molecular spectroscopy," Am. J. Phys. 80(8), 664–669 (2012).

⁶J. C. Williamson, T. S. Kuntzleman, and R. A. Kafader, "A molecular iodine spectral data set for rovibronic analysis," J. Chem. Educ. 90(3), 383-385 (2013).

⁷S. B. Bayram and M. V. Freamat, "A spectral analysis of laser induced fluorescence of diatomic iodine," in American Association of Physics Teachers, 2015.

⁸S. B. Bayram, M. Freamat, and P. T. Arndt, "Rotational spectra of N₂⁺: An undergraduate laboratory in atomic and molecular spectroscopy," Am. J. Phys. 83(10), 867–872 (2015).

- ⁹D. C. Lincoln, D. DeMille, R. V. Krems, and J. Ye, "Cold and ultracold molecules: Science, technology and applications," New J. Phys. 11, 055049 (2009).
- ¹⁰H.-K. Chung, K. Kirby, and J. F. Babb, "Theoretical study of the absorption spectra of the sodium dimer," Phys. Rev. A 63(3), 032516 (2001).
- ¹¹W. Demtröder, M. McClintock, and R. N. Zare, "Spectroscopy of Na₂ using laser-induced fluorescence," J. Chem. Phys. **51**(12), 5495–5508 (1969).
- ¹²P. Kusch and M. M. Hessel, "Perturbations in the A $^{1}\Sigma_{u}^{+}$ state of Na₂," J. Chem. Phys. **63**(9), 4087–4088 (1975).
- ¹³R. H. Callender, J. I. Gersten, R. W. Leigh, and J. L. Yang, "Laser-induced atomic fluorescence from Na₂," Phys. Rev. A 14(5), 1672–1682 (1976).
- ¹⁴W. Demtröder and M. Stock, "Molecular constants and potential curves of Na₂, from laser-induced fluorescence," J. Mol. Spectrosc. 55(1-3), 476–486 (1975).
- ¹⁵O. Babaky and K. Hussein, "The ground state X $^{1}\Sigma_{g}^{+}$ of Na₂," Can. J. Phys. **67**(9), 912–918 (1989).
- ¹⁶S. Magnier, Ph Millie, O. Dulieu, and F. Masnou-Seeuws, "Potential curves for the ground and excited states of the Na₂ molecule up to the (3s+5p) dissociation limit: Results of two different effective potential calculations," J. Chem. Phys. **98**(9), 7113–7125 (1993).
- ¹⁷M. Born and J. R. Oppenheimer, "On the quantum theory of molecules," Ann. Phys. **389**(20), 457–484 (1927).
- ¹⁸P. M. Morse, "Diatomic molecules according to the wave mechanics. II. Vibrational levels," Phys. Rev. 34(1), 57–64 (1929).
- ¹⁹Peter F. Bernath, Spectra of Atoms and Molecules, 3rd ed. (Oxford University Press, New York, 2016).
- ²⁰W. Demtröder, *Laser Spectroscopy* 2, 5th ed. (Springer, London, 1983).
- ²¹E. U. Condon, "The Franck-Condon principle and related topics," Am. J. Phys. 15(5), 365–374 (1947).
- ²²G. Lucchese, R. R. Lucchese, and S. W. North, "A new java program for graphical illustration of the Franck Condon principle: Application to the I₂ spectroscopy experiment in the undergraduate physical chemistry laboratory," J. Chem. Educ. 87(3), 345–345 (2010).
- ²³R. J. Le Roy, "Level 8.0: A computer program for solving the radial Schrödinger equation for bound and quasibound levels, Guelph-Waterloo Centre for graduate work in chemistry." Technical Report No. CP-663 (University of Waterloo, Waterloo, Ontario, Canada, 2007).
- ²⁴R. J. Le Roy, "LEVEL: A computer program for solving the radial Schrödinger equation for bound and quasibound levels," J. Quant. Spectrosc. Radiat. Transfer 186, 167–178 (2017).
- ²⁵H. Richter, H. Knöckel, and E. Tiemann, "The potential of the Na₂ $B^1\Pi_u$ state," J. Chem. Phys. **157**, 217–229 (1991).
- ²⁶P. Kusch and M. M. Hessel, "An analysis of the $B^1\Pi_u X^1\Sigma_g^+$ band system of Na₂," J. Chem. Phys. **68**(6), 2591–2606 (1978).
- ²⁷A. A. Radzig and B. M. Smirnov, Reference Data on Atoms, Molecules, and Ions (Springer-Verlag, Berlin, Heidelberg, 1985).
- ²⁸P. T. Arndt, V. B. Sovkov, J. Ma, X. Pan, D. S. Beecher, J. Y. Tsai, R. Livingston, V. M. Marcune, A. M. Lyyra, and E. H. Ahmed, "Experimental study of the 3 $^3\Pi_g$ and 4 $^3\Sigma_g^+$ states of the rubidium dimer," Phys. Rev. A **105**(3), 032823 (2022).
- ²⁹P. W. Atkins, *Molecular Quantum Mechanics*, 2nd ed. (Oxford University Press, Oxford, Great Britain 1983).
- ³⁰G. Herzberg, Molecular Spectra and Molecular Structure (D. van Nostrand Company, Inc. Princeton, NJ, 1950).
- ³¹I. Duck and E. C. G. Sudarshan, "Toward an understanding of the spinstatistics theorem," Am. J. Phys. 66(4), 284–303 (1998).

- ³²C. R. Vidal and J. Cooper, "Heat-pipe oven: A new, well-defined metal vapor device for spectroscopic measurements," J. Appl. Phys. 40(8), 3370–3374 (1969).
- ³³C. R. Vidal and F. B. Haller, "Heat pipe oven applications. I. Isothermal heater of well defined temperature. II. Production of metal vapor-gas mixtures," Rev. Sci. Instrum. 42(12), 1779–1784 (1971).
- ³⁴C. R. Vidal and M. M. Hessel, "Heat-pipe oven for homogeneous mixtures of saturated and unsaturated vapors; application to NaLi," J. Appl. Phys. 43(6), 2776–2780 (1972).
- ³⁵D. Hite, M. Deebel, E. Thoreson, C. Lengacher, R. E. Miers, and M. F. Masters, "Construction of a heat pipe oven on a small budget," Am. J. Phys. 65(10), 1017–1022 (1997).
- ³⁶T. T. Grove, W. A. Hockensmith, N. Cheviron, W. Grieser, R. Dill, and M. F. Masters, "Construction of an inexpensive copper heat-pipe oven," Eur. J. Phys. 30(6), 1229–1237 (2009).
- ³⁷P. Todorov, T. Vartanyan, C. Andreeva, D. Sarkisyan, G. Pichler, and S. Cartaleva, "High resolution laser spectroscopy of spatially restricted hot alkali atomic and dimer vapor," Opt. Quantum Electron. 52, 1–12 (2020).
- ³⁸D. Sarkisyan, T. Varzhapetyan, A. Sarkisyan, Yu Malakyan, A. Papoyan, A. Lezama, D. Bloch, and M. Ducloy, "Spectroscopy in an extremely thin vapor cell: Comparing the cell-length dependence in fluorescence and in absorption techniques," Phys. Rev. A 69(6), 065802 (2004).
- ³⁹A. N. Nesmeyanov, Vapor Pressure of the Elements (Academic Press, New York, 1963), Vol. 87, p. 345.
- ⁴⁰MGL-III-532-20mW. This BBDL was bought ten years ago from <www.optoengine.com>, and current price is about \$2k. However, similar laser, PGL-VI-532, with the same output power is currently \$300. The NBDL is a 10-W Coherent Verdi with 5 MHz linewidth.
- ⁴¹USB4000-UV-VIS spectrometer. This spectrometer, bought from Ocean Optics, is no longer available since the company was bought by <www.oceaninsight.com>; the alternative spectrometer (Flame UV-VIS) price is listed as \$3931. On the other hand, <www.thorlabs.com> has a similar compact spectrometer (CCS100) with a current price of \$2,211.69.
- ⁴²NIST, https://physics.nist.gov/PhysRefData/Handbook/element_name.htm
- ⁴³See supplementary material online for the Franck-Condon factors involved in the experiment.
- ⁴⁴R. T. Birge and H. Sponer, "The heat of dissociation of non-polar molecules," Phys. Rev. 28(2), 259–283 (1926).
- ⁴⁵L. Lessinger, "Morse oscillators, Birge-Sponer extrapolation, and the electronic absorption spectrum of I₂," J. Chem. Educ. 71(5), 388–391 (1994).
- ⁴⁶K. M. Jones, S. Maleki, S. Bize, P. D. Lett, C. J. Williams, H. Richling, H. Knöckel, E. Tiemann, H. Wang, P. L. Gould, and W. C. Stwalley, "Direct measurement of the ground-state dissociation energy of Na₂," Phys. Rev. A 54(2), R1006–R1009 (1996).
- ⁴⁷W. C. Stwalley, "RKR potential curves directly from a single resonance fluorescence doublet series," J. Chem. Phys. **56**(5), 2485–2486 (1972).
- ⁴⁸R. J. LeRoy, "Molecular constants and internuclear potential of ground-state molecular iodine," J. Chem. Phys. **52**(5), 2683–2689 (1970).
- ⁴⁹F. Castanō, J. de Juan, and E. Martinez, "The calculation of potential energy curves of diatomic molecules: the RKR method," J. Chem. Educ. **60**(2), 91–93 (1983).
- ⁵⁰W. C. Stwalley, "Up and away in the potential landscape of diatomic molecule potential energy curves," J. Mol. Spectrosc. 330, 14–19 (2016).
- ⁵¹J. Katriel, "An undergraduate-oriented comment about inverting spectral data to determine the interatomic potential," Am. J. Phys. 88(12), 1147–1150 (2020).